

18th CIRP Conference on Modeling of Machining Operations

Material parameter optimization for orthogonal cutting simulations of AISI4140 at various tempering conditions

Benedict Stampfer^{a,*}, Germán González^a, Eric Segebade^a, Michael Gerstenmeyer^a and Volker Schulze^a

^awbk Institute of Production Science, Karlsruhe Institute of Technology (KIT), Kaiserstr. 12, 76131 Karlsruhe, Germany

* Corresponding author. Tel.: +49-721-608-42455; fax: +49-721-608-45004. E-mail address: benedict.stampfer@kit.edu

Abstract

The mechanical parameters of quenched and tempered AISI4140 and the machining process characteristics are depending on the material's tempering state. The process characteristics of practical relevance are not only the cutting forces and the tool wear, but also the surface layer states of the machined part. In order to predict and to improve these characteristics efficiently, chip forming simulation via finite element method (FEM) is commonly applied. However, an issue in machining simulation which is often addressed is choosing appropriate material parameters for the flow stress model. This especially accounts for AISI4140 with various tempering conditions, as in many cases the precise heat treatment is not supplied in detail, even in scientific literature.

In this work, orthogonal cutting of AISI4140 with tempering temperatures of 300°C, 450°C and 600°C is investigated by experiments and FE simulations. The Johnson-Cook flow stress model is used in the FE simulation. The referring material parameters for the tempering conditions are iteratively adapted via numerical optimization to fit experimental cutting forces. The obtained parameters are compared to literature values in order to prepare a common ground for the cutting simulation of AISI4140. This contributes to an enhanced process modelling when machining AISI4140 with use-case adapted heat treatments.

© 2021 The Authors. Published by Elsevier B.V.

This is an open access article under the CC BY-NC-ND license (<https://creativecommons.org/licenses/by-nc-nd/4.0>)

Peer-review under responsibility of the scientific committee of the 18th CIRP Conference on Modeling of Machining Operation.

Keywords: Cutting; heat treatment; modeling;

1. Introduction

Numerical modeling of machining is desired for many reasons. One of those is surface engineering, which requires exhaustive experimental and metallographic analyses. A Finite Element (FE) simulation could reduce involved efforts, but this requires amongst others the knowledge of the flow stress curve of the machined material.

The starting point of this work is the need for a robust identification method for material flow stress parameters regarding multiple levels of machining experiments, multiple target values and multiple tempering states. The material regarded is AISI4140, which was quenched and subsequently tempered for 1 h with alternative temperatures of 300°C, 450°C

and 600°C, denoted as QT 300, QT 450 and QT 600. The latter represents the delivered condition according to DIN EN 10083, while the other heat treatments are applied when a higher hardness or a higher strength is required.

A widely used modeling approach for the equivalent flow stress σ_f in machining is the Johnson-Cook equation [1]:

$$\sigma_f = [A + B \bar{\epsilon}^n] \left[1 + C \ln \left(\frac{\dot{\bar{\epsilon}}}{\dot{\bar{\epsilon}}_0} \right) \right] \left[1 - \left(\frac{\theta - \theta_0}{\theta_m - \theta_0} \right)^m \right] \quad (1)$$

Herein $\bar{\epsilon}$ denotes the accumulated plastic strain, $\dot{\bar{\epsilon}}$ the equivalent plastic strain rate, $\dot{\bar{\epsilon}}_0$ the reference plastic strain rate, θ the material temperature, θ_m the material's melting temperature and θ_0 the room temperature. Coefficient A is the yield strength, B is the hardening modulus, C is the strain rate

sensitivity coefficient, n is the hardening coefficient and m is the thermal softening coefficient. The calibration of flow stress parameters is a difficult task because machining strains, strain rates and temperatures are not reached in conventional material characterization tests. Özel and Zeren [2] addressed this issue by combining material and machining test data, as well as Oxley's analytical shear zone model [3] in order to numerically optimize the flow stress and the friction parameters in metal machining. Storchak et al. [4] used this combined approach and compared it to an optimization solely based on material tests. With a process force residuum of 8 % to 18 % for the machining of AISI 1045 and Ti-1023, the combined approach resulted in a superior prediction. Yet the approach is not pursued in this work, because it would require material characterization tests for each regarded heat treatment state of AISI 4140.

Bort et al. [5] simulated orthogonal cutting of AISI 304 and optimized the Johnson-Cook flow stress parameters as well as the shear friction factor by the Downhill Simplex Algorithm (DSA). The cutting force, the chip thickness, the contact length and the curvature of one experiment were used as optimization target values. Bosetti et al. [6] continued the work of [5] and investigated the effect of the initialization on the optimization procedure. The initial flow stress parameters were generated randomly, by a generic algorithm or chosen according to values in the literature. An obligatory subsequent DSA resulted in a good cutting force prediction, irrespective of the initial values. The flow stress parameters originating from the random initialization incorporated a physically unlikely yield strength of 118 MPa, compared to 530 MPa for the literature approach and 634 MPa for the generic approach, i.e. the optimization problem is characterized by multiple minima. Regarding the computational efficiency, the generic preconditioning required high efforts. Still the algorithm did not lead to superior target function values, but was used in conjunction with DSA.

Eisseler et al. [7] used a Design of Experiments approach to identify Johnson-Cook flow stress parameters for orthogonal cutting of AISI 4142. The cutting force residuum was reduced for one set of cutting parameters with one material state. The main disadvantage of this approach is the high number of iterations, as it relies on latin hypercube sampling and doesn't feature an inherent convergence behavior.

Agmell et al. [8] used a Kalman filter approach to optimize the Johnson-Cook flow stress parameters of orthogonal cutting. The thereby reached agreement of the cutting forces and the chip compression ratios is high. However the approach was limited to one level of cutting experiments, whereas a multilevel optimization is aspired in the present work.

Bergs et al. [9] presented the numerical optimization of Johnson-Cook flow stress parameters for orthogonal cutting of normalized AISI 1045 by a modified DSA. The target function incorporated the process forces, the chip thickness and the chip temperature. The yield strength was experimentally determined and kept constant. Three levels of cutting test were used for the parameter optimization. This resulted in a fair agreement of the target values, excluding the passive forces, which were strongly underestimated by the simulation.

Bäker [10] presented an efficient method to optimize flow stress parameters. It is carried out by solving equations, which originally result from FE simulations, while neglecting second

order effects of the parameter variation. Subsequently the full effect of the thus identified parameters on the target values is tested by a machining simulations and the procedure is repeated until convergence is reached. The ambiguity of Johnson-Cook parameters in machining simulations is mentioned but remains an unsolved issue.

The literature review up to this point shows the applicability of the DSA for the Johnson-Cook parameter optimization in cutting simulations and the importance of physically reasonable initial values or parameter intervals for the regarded workpiece material, in this case AISI4140. Papers which contribute thereto are reviewed in the following sections.

Arrazola et al. [11] experimentally and numerically analyzed the sensitivity of chip formation mechanisms to longitudinal turning parameters. As workpiece material a rather soft AISI4140 was used (262 - 293 HB), which was represented in the FE simulations by the Johnson-Cook flow stress model. While receiving a good agreement of the chip geometry and the cutting force, the simulated feed forces surpass the experimental ones by more than 50 %. Due to this lack of agreement the used Johnson-Cook parameters were not chosen as a starting point for the present work.

Agmell et al. [12] also simulated orthogonal cutting of AISI4140 by means of the Johnson-Cook flow stress model. A wide range of cutting thickness parameters was regarded in simulations and compared to experiments, leading to a good agreement for both, cutting and passive forces. Rami et al. [13] successfully used the Johnson-Cook flow stress parameters of [12] to simulate residual stresses after turning of AISI4140 with a low hardness. Thus these flow stress parameters were chosen as initial values for the optimization algorithm of this work.

Buchkremer and Klocke [14] investigated orthogonal cutting of AISI4140 QT with a tempering temperature of 400°C, using the Johnson-Cook flow stress model. The parameters A , B and n were identified by tensile tests, while C and m were calibrated in order to fit the cutting power, the force ratio and the chip thickness of four levels of cutting tests. The experimental trends of those targets were met by the simulation. Thus the flow stress parameters were chosen as alternative initial values for the optimization algorithm.

The DSA was engaged in this work, because it features many benefits, e.g. its numerical derivation capability of the target function, which leads to a good local convergence behavior, the moderate use of computational resources and the simplicity and thus traceability of the algorithm. Focusing on surface engineering and the workpiece loads, the chip geometry is not analyzed here, but the passive force will be regarded, as it acts normal on the machined surface. An issue of the Johnson-Cook parameter identification for machining simulations is the apparent ambiguity of the derived solution. This is addressed by the consideration of multiple experimental levels during the optimization procedure.

2. Experimental Setup

Orthogonal dry turning tests were conducted on a vertical CNC turning machine of the type Index V100 with TiCN-coated carbide tools of the type Walter CCMW120404-RK6 WKK10S. Those were used to cut circular AISI4140 specimen

of the diameter 49 mm to an end diameter of 26 mm. The fixed process parameters were the rake angle $\gamma = 0^\circ$, the clearance angle $\alpha = 7^\circ$, the width of cut b was 4 mm, the cutting volume of 5419 mm³ and the cutting edge radius of $r_\beta = 50 \mu\text{m}$, measured using a perthometer. The values of fully factorial varied process parameters are specified in Figure 2.

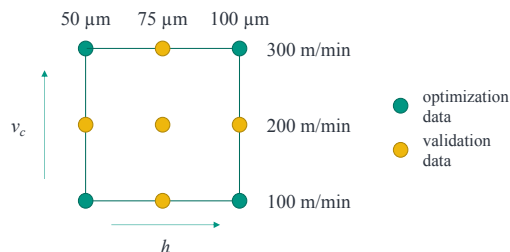


Figure 1. Process parameters of the orthogonal turning tests conducted with AISI4140 QT 300, QT 450 and QT 600.

Herein v_c denotes the cutting velocity and h the cutting thickness. The tests were conducted for the material states AISI4140 QT 300, QT 450 and QT 600. Figure 2 also indicates which data was used during the optimization procedure and for the validation of the resulting flow stress parameters.

The process forces were measured by a Kistler 9257B dynamometer with a channel frequency of 2000 Hz. The tool temperatures were measured with three type N thermocouples of the diameter 0.5 mm and a channel frequency of 100 Hz at the positions, which are given in Figure 2. The channels for the thermocouples were manufactured by Electrical Discharge Machining.

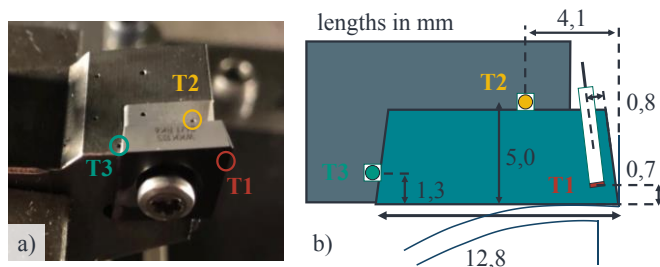


Figure 2. Cutting tool and thermocouple positions: (a) Picture, (b) top view sketch, cross-section in the mid cutting plane.

The forces and the tool temperatures were evaluated at the end of the cutting process, because those thermal and mechanical loads are relevant for surface modifications. The tool temperatures were not regarded as target values for the optimization. Instead they were used to derive thermal boundary conditions for the interface between the insert and the tool holder in the FE simulations, which is explained the next chapter.

3. Numerical model

3.1. FE model

The FE simulations were conducted with the software Simufact Forming 16.0, which is based on MSC Marc 2018. For the modelling of the workpiece material, the von Mises

plasticity and the Johnson-Cook flow stress equation were used. Orthogonal turning was simulated as a two dimensional process with a plain strain assumption and an explicit time integration. Furthermore an Arbitrary Lagrange Eulerian formulation with a frequent workpiece remeshing was used, which resulted in a minimum element edge length of 8 μm . Constant parameters of the FE model summarized in Table 1.

Table 1. Parameters of the FEM Simulation.

inc	l_c	α_{air}	θ_0	θ_m	$\dot{\bar{\epsilon}}$
-	μm	W/(m ² K)	K	K	-
200	500	50	293	1820	1

After approximately one third of the time increments inc and the length of cut l_c , the run-in of the process forces and the chip geometry was completed. The remeshing was triggered by an element strain change of 0.4, which was usually reached after a period of eight time increments. α_{air} denotes the heat transfer coefficient between the tool or the workpiece and the environment, θ_0 represents the environmental temperature, as well as the reference temperature for the Johnson-Cook flow stress model, θ_m the melting temperature and $\dot{\bar{\epsilon}}$ the reference strain rate, see Eq. (1).

The tool workpiece contact was modeled by Eq. (2). Herein τ_f denotes the contact shear stress, σ_n the contact normal stress, μ the coulomb friction coefficient and τ the shear friction coefficient.

$$\tau_f = \begin{cases} \mu * \sigma_n & \text{when } \mu * \sigma_n < \sigma_f \\ \tau * \sigma_f & \text{when } \mu * \sigma_n > \sigma_f \end{cases} \quad (2)$$

The combined friction model was amongst others used by [12]. In this work the coulomb coefficient was set to $\mu = 0.3$ and the shear coefficient to $\tau = 1$. An interesting aspect of this model is, that the contact stresses are directly dependent on the flow stress parameters, which should be beneficial for the parameter optimization. The coulomb friction coefficient is sometimes modeled as function of the sliding velocity, which usually decreases the friction [14, 15]. This is neglected, because one goal of this work is to explore the abilities and limitations of optimized Johnson-Cook flow stress parameters.

To reach the thermal conditions at the end of the cutting tests within the simulations, the tool's specific heat capacity was reduced, which was proposed by Lorentzon and Järvesträt [16]. The tool temperatures measured according to Figure 2 were extrapolated into a temperature field by a thermal steady state simulation of the insert only. Thereafter the insert edge temperatures were extracted and defined in the cutting simulation as Dirichlet boundary condition. The respective insert edge is marked yellow in Figure 3 (a). Figure 3 (b) gives an impression of the mesh refinement in the tool and the workpiece.

The microgeometry of the cutting edge used in the presented FE simulations is depicted in Figure 3 (c). The geometry was CAD-generated by horizontally trimming the clearance face of an ideal cutting edge with the radius 50 μm . This was done, because the FE simulation with an ideally round edge resulted in a flank workpiece contact length of 50 to 60 μm . However microscopic records of the tool flank indicate a contact length

of 70 μm or more, even for unworn tools. This is attributed to the fact that the coated cutting tool is not fully characterized by a perfect radius. By horizontally trimming the FE model of the insert, the simulated tool workpiece contact lengths matched approximately for all experiments. This simple approach was chosen, because the focus of this work is not the identification and analysis of tool microgeometries.

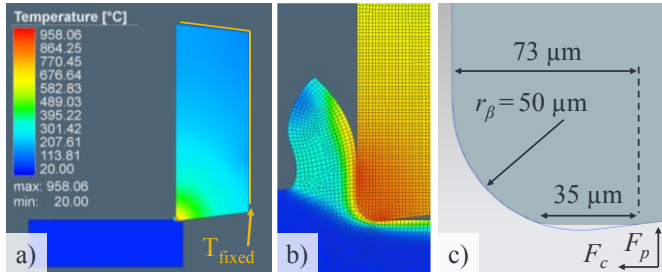


Figure 3. (a) FE model and prescription of insert boundary temperatures (b) process zone and detailed mesh (c) cutting edge microgeometry.

3.2. Optimization procedure

The optimization was run independently for AISI4140 QT 300, QT 450 and QT 600. In Figure 2, the cutting parameter set chosen for the optimization is depicted. In a first step, the input files of the simulations were generated with Simufact Forming. Thereafter the .dat input-file of each simulation was modified, so that it reads the flow stress parameters from an external file. The optimization procedure is started by a main script implemented in Matlab R2020a. Within this, the function *fminsearch* is called, which is basically taking the initial Johnson-Cook parameters and calls the user written *target function script*. The script copies the received Johnson-Cook parameters into a text file, which serves as additional input for the FE-model and starts the thus prepared simulations in a parallel for-loop. After completing the simulations, the process forces are compared to the experimental values by the actual target function, which is given by:

$$\Delta F = \sum_{i=1}^4 \sqrt{(F_{c,exp,i} - F_{c,sim,i})^2 + (F_{p,exp,i} - F_{p,sim,i})^2} \quad (3)$$

Herein ΔF is the accumulated deviation of the process forces, which should be minimized, i is the index of the optimization parameter set and F_{exp} and F_{sim} denote the experimental and the simulated cutting forces.

The *target function script* returns the accumulated deviation to *fminsearch*, which generates a new set of flow stress parameters by performing the DSA. Thereafter *fminsearch* returns the new set of flow stress parameters to the *target function script*. In the optimization runs for this paper, the maximum number of DSA iterations was set to 50. Practically the target function values presented in the next chapter were usually derived after less than 25 iterations.

As auxiliary quantity for the force deviation evaluation the accumulated experimental forces are defined as:

$$F_{sum,exp} = \sum_{i=1}^4 \sqrt{F_{c,exp,i}^2 + F_{p,exp,i}^2} \quad (4)$$

For the material states AISI4140 QT 600, QT 450 and QT 300 this resulted in the values 4301 N, 4786 N and 5821 N. Thereby the force deviation can be normalized according to:

$$\Delta F_n = \Delta F / F_{sum,exp} \quad (5)$$

4. Results and Discussion

The first optimization runs were conducted with the initial parameters identified in [12]. The resulting flow stress parameters and the normalized force deviations are presented in Table 2.

Table 2. Flow stress parameters and accumulated force deviations resulting from DSA with initial values of [12].

parameter	A	B	C	m	n	ΔF_n
unit	MPa	MPa	-	-	-	%
Start [12]	595.0	580.0	0.023	1.03	0.133	-
QT 600	637.75	608.14	0.0241	0.9193	0.1352	4.3
QT 450	722.23	659.30	0.0255	0.9499	0.0912	3.4
QT 300	1312.0	1091.6	0.0231	0.4105	0.0776	5.4

The force deviations can be considered very low. The flow stress parameters of AISI4140 QT 600 are close to the initial values. The identified yield strength of AISI4140 QT 450 is higher than those of QT 600, which is plausible as well. Still one would expect even higher values, considering that in [14] a yield strength of 1450 MPa was identified for a tempering with 400 °C. The optimized material parameters of Table 2 were used for the simulation of the complete process parameter field.

In Figure 4 and Figure 5, the simulated and experimental machining forces of AISI4140 QT 600 are depicted. The experimental optimization and validation data is predicted equally well. Furthermore, the evolution of the experimental forces with the cutting thickness is predicted fully satisfactory. While the experimental cutting forces significantly decrease with the cutting velocity, the trend is less pronounced in the simulation. Besides, the decreasing trend of the experimental passive forces is not present in the simulations. A possible explanation is, that the coefficient of friction decreases with the sliding velocity [15], while it was kept constant in the present simulations.

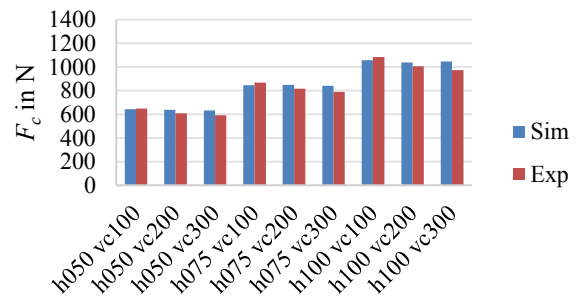


Figure 4. Cutting force comparison of AISI4140 QT 600 with optimized flow stress parameters according to Table 2.

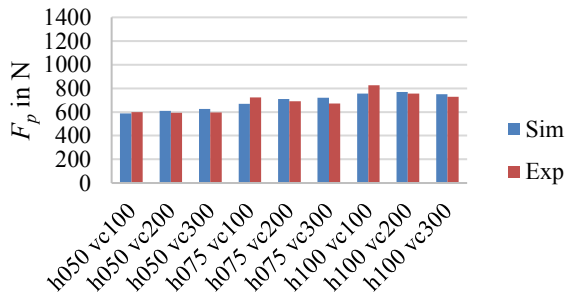


Figure 5. Passive force comparison of AISI4140 QT 600 with optimized flow stress parameters according to Table 2.

The comparison of simulated and experimental process forces of AISI4140 QT 450 is given in Figure 6 and Figure 7. The experimental optimization and validation data is predicted equally well. Furthermore, the evolution of the experimental forces with the cutting thickness is predicted fully satisfactory. While the decreasing trend of the cutting forces with the cutting velocity is hardly met in the simulation, the increasing trend of the experimental passive forces with the cutting velocity is generally present.

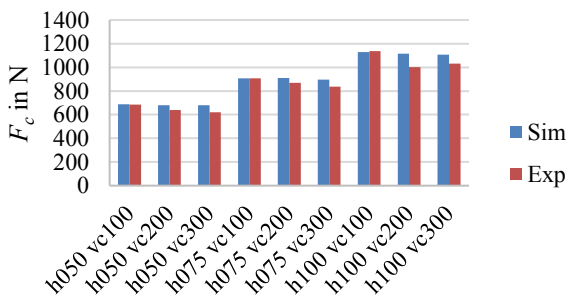


Figure 6. Cutting force comparison of AISI4140 QT 450 with optimized flow stress parameters according to Table 2.

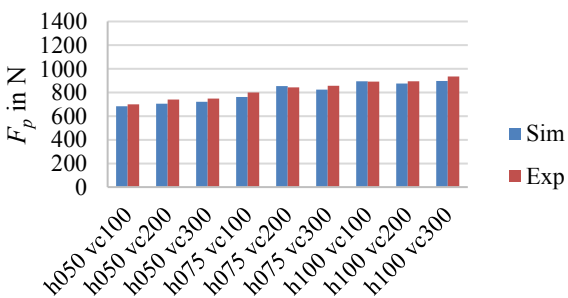


Figure 7. Passive force comparison of AISI4140 QT 450 with optimized flow stress parameters according to Table 2.

The machining forces of AISI4140 QT 300 are depicted in Figure 8 and Figure 9. Compared the previously regarded material states, the decreasing trend of the experimental cutting forces with the cutting velocity is developed stronger. Besides this, the general level of cutting forces is hardly increased, compared to the other material states. The experimental passive forces however almost double, when comparing AISI4140

QT 600 with QT 300. It can be concluded that the material's hardness primary affects the normal forces on the tool flank. This further indicates that the workpiece flank contact length is of high importance for a good passive force prediction, especially for hard workpiece materials. Regarding the process parameters sets for optimization and validation, the forces are simulated equally well. Furthermore the evolution of the forces with the cutting thickness is predicted satisfactorily. Regarding the experimental force evolution with the cutting velocity, the cutting force decreases and the passive force increases. Those trends are not met by the simulation. Generally, it is hard to imagine that a change of flow stress curve may lead to an increase in one force component and a decrease in the other. Additional simulations show that the ratio of cutting and passive forces can be changed by the coulomb friction coefficient. Given that the friction changes with the cutting velocity, an opposing course of the force components can be imagined.

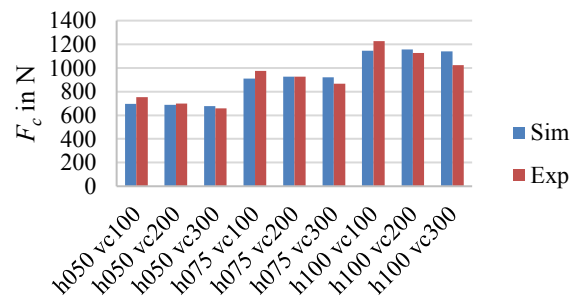


Figure 8. Cutting force comparison of AISI4140 QT 300 with optimized flow stress parameters according to Table 2.

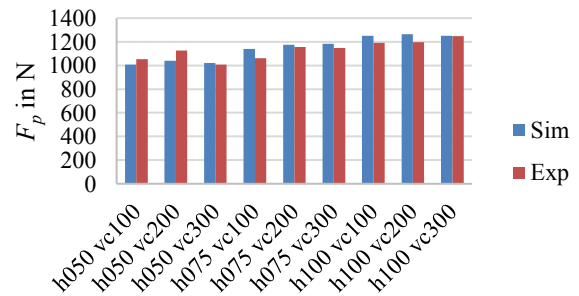


Figure 9. Passive force comparison of AISI4140 QT 300 with optimized flow stress parameters according to Table 2.

The optimization was also conducted with the initial material parameters identified in [14]. In Table 3 the resulting flow stress parameters and normalized force deviations are presented. The force deviations are low and similar to those of Table 2. This indicates that the differences between the forces simulated with the alternatively optimized parameter sets must be low as well. Hence the comparison of individual process forces is not repeated at this point. The low force deviations in Table 2 and Table 3 reflect the ability of the DSA to find equivalent minima in the target function, when starting from different initial values. However the identified flow stress parameters can be fundamentally different. This shows that the

ambiguity issue of the Johnson-Cook flow stress parameters is not solved reliably by regarding multiple machining levels.

The determined yield strengths in Table 3 are higher than in Table 2. This makes the parameter sets in Table 3 for AISI4140 QT 450 and QT 300 more convincing from a physical point of view and shows that the presented optimization method leads to good results, given suitable initial parameters. Alternatively the easily accessible yield strength could be taken as fixed value.

Table 3. Flow stress parameters and accumulated force deviations resulting from DSA with initial values [14].

parameter	A	B	C	m	n	ΔF_n
unit	MPa	MPa	-	-	-	%
Start [10]	1450.0	910.0	0.034	0.328	0.450	-
QT 600	1232.5	988.66	0.0362	0.2913	0.4896	4.0
QT 450	1485.1	939.54	0.0352	0.3210	0.4404	3.4
QT 300	1743.4	852.15	0.0392	0.3605	0.3097	6.8

In further works the machining simulation should be used for the prediction of surface states. Considering that phase transformations and recrystallization processes are to a large extent temperature driven, the thermal process modelling is going to be relevant. Thus respective assumptions are analyzed, based on the measured tool temperatures. Regarding the thermocouple T1, the predicted temperatures are in the range of 390 °C to 570 °C and increase with both, the cutting velocity and the cutting thickness. Those temperatures are not correlated to the material state, which indicates that the optimization is independent from the tool temperatures. The experimentally measured temperatures are in the range of 270 °C to 365 °C. The overestimation of the tool temperatures in the simulation can have many reasons, e.g. the neglect of a heat flow normal to the cutting plane or too high friction coefficients between tool and workpiece. However the main point is, that in contrast to the simulation the tool didn't reach a thermal steady state in the experiment, despite a cutting volume of 5419 mm³. This is confirmed by the slope of the thermocouple runs at the process end. Consequently the heat capacity of the tool shouldn't be reduced to nearly zero, as done in the presented model, but must be reduced in such a way that the tool heats up adequately during the simulation, with respect to the experimental cutting length.

5. Conclusion

The presented results prove the applicability of the DSA for the multi-parameter level identification of Johnson-Cook flow stress parameters. The absolute and relative agreement of the process forces is very good. However, some minor trends are difficult to predict, e.g. when the passive force increases with the cutting velocity, while the cutting force decreases. A promising approach to improve this could be to model cutting velocity sensitive thermal and frictional effects more precisely. Generally, the good agreement of the measured and simulated process forces are a solid ground for the modeling of surface integrity, such as residual stresses, grain refinement or phase

transformations. The simulation of the transient tool heating and the application of the optimization method to surface integrity models will be studied in future works.

Acknowledgements

The scientific work has been supported by the DFG within the research priority program SPP 2086 (SCHU 1010/63-1 and SCHU 1010/65-1). The authors thank the DFG for this funding and intensive technical support.

References

- [1] Johnson GR, Cook WH. A constitutive model and data for metals subjected to large strains, high strain and high temperatures. In: Proceedings of the 7th International Symposium on Ballistics, The Hague, The Netherlands, 1983: 541-547.
- [2] Özel, T.; Zeren, E. A Methodology to Determine Work Material Flow Stress and Tool-Chip Interfacial Friction Properties by Using Analysis of Machining. ASME J. Manuf. Sci. Eng. 128, 2006: 119-129.
- [3] Oxley, P. L. B., 1989, Mechanics of Machining, an Analytical Approach to Assessing Machinability, Ellis Horwood Limited.
- [4] Storchak, M.; Rupp, P.; Möhring, H.-C.; Stehle, T.: Determination of Johnson-Cook constitutive parameters for cutting simulations. Metals 9, 2019: 473.
- [5] Bort CG, Bruschi S, Bosetti P. Johnson Cook Parameter Identification for AISI-304 Machining Through Nelder-Mead Method. In: Proceedings of the XI International Conference on Computational Plasticity Fundamentals and Applications, 2011: 1-12.
- [6] Bosetti P, Giorgio Bort CM, Bruschi S. Identification of Johnson-Cook and Tresca's Parameters for Numerical Modeling of AISI-304 Machining. In: Processes Journal of Manufacturing Science and Engineering 135, 2013: 051021.
- [7] Eisseler, R.; Drewle, K.; Grötzing, K.; Möhring, H.-C. Using an inverse cutting simulation-based method to determine the Johnson-Cook material constants of heat-treated steel. Procedia CIRP 77, 2018: 26-29.
- [8] Agmell M, Ahadi A, Ståhl J-E. Identification of plasticity constants from orthogonal cutting and inverse analysis. In: Mechanics of Materials 77, 2014: 43-51.
- [9] Bergs T, Hardta M, Schrakneppera D. Determination of Johnson-Cook material model parameters for AISI 1045 from orthogonal cutting tests using the Downhill-Simplex algorithm. In: Procedia Manufacturing 48, 2020: 541-552.
- [10] Bäker, M. A new method to determine material parameters from machining simulations using inverse identification. Procedia CIRP 31, 2015: 399-404.
- [11] Arrazola PJ, Villar A, Ugarte D, Marya S. Serrated chip prediction in finite element modeling of the chip formation process. In: Machining Science and Technology 11 (3): 367-390.
- [12] Agmell M, Ahadi A, Ståhl J-E. A fully coupled thermomechanical two-dimensional simulation model for orthogonal cutting: formulation and simulation. In: Proc. IMechE J. Engineering Manufacture 225, 2011: 1735-1745.
- [13] Rami A, Kallel A, Sghaier S, Youssef S, Hamdi H. Residual stresses computation induced by turning of AISI 4140 steel using 3D simulation based on a mixed approach. In: Int J Adv Manuf Technol 91, 2017: 3833-3850.
- [14] Buchkremer S, Klocke F. Compilation of a thermodynamics based processsignature for the formation of residual surface stresses in metal cutting. In: Wear 376-377, 2017: 1156-1163.
- [15] Rech J, Arrazola PJ, Claudin C, Courbon C, Pusavec F, Kopac J. Characterisation of friction and heat partition coefficients at the tool-work material interface in cutting. CIRP Annals - Manufacturing Technology 62, 2013: 79-82.
- [16] Lorentzon J, Järvstråt N. Modelling tool wear in cemented-carbide machining alloy 718. In: International Journal of Machine Tools and Manufacture 48 (10). 2008: 1072-1080.